


Article

Drought-Induced Mortality Is Related to Hydraulic Vulnerability Segmentation of Tree Species in a Savanna Ecosystem

Shubin Zhang ^{1,2,3,*} , Guojing Wen ^{1,3} and Daxin Yang ^{1,3}

¹ CAS Key Laboratory of Tropical Forest Ecology, Xishuangbanna Tropical Botanical Garden, Chinese Academy of Sciences, Mengla 666303, Yunnan, China

² Graduate School of Agriculture, Kyoto University, Kitashirakawa Oiwake-Cho, Kyoto 606-8502, Japan

³ Yuanjiang Savanna Ecosystem Research Station, Xishuangbanna Tropical Botanical Garden, Chinese Academy of Sciences, Yuanjiang 653300, Yunnan, China

* Correspondence: zhangshubin@xtbg.ac.cn; Tel.: +86-691-871-3046; Fax: +86-691-871-5070

Received: 21 June 2019; Accepted: 15 August 2019; Published: 17 August 2019



Abstract: Vulnerability segmentation (VS) has been widely suggested to protect stems and trunks from hydraulic failure during drought events. In many ecosystems, some species have been shown to be non-segmented (NS species). However, it is unclear whether drought-induced mortality is related to VS. To understand this, we surveyed the mortality and recruitment rate and measured the hydraulic traits of leaves and stems as well as the photosynthesis of six tree species over five years (2012–2017) in a savanna ecosystem in Southwest China. Our results showed that the NS species exhibited a higher mortality rate than the co-occurring VS species. Across species, the mortality rate was not correlated with xylem tension at 50% loss of stem hydraulic conductivity ($P_{50\text{stem}}$), but was rather significantly correlated with leaf water potential at 50% loss of leaf hydraulic conductance ($P_{50\text{leaf}}$) and the difference in water potential at 50% loss of hydraulic conductance between the leaves and terminal stems ($P_{50\text{leaf-stem}}$). The NS species had higher Huber values and maximum net photosynthetic rates based on leaf area, which compensated for a higher mortality rate and promoted rapid regeneration under the conditions of dry–wet cycles. To our knowledge, this study is the first to identify the difference in drought-induced mortality between NS species and VS species. Our results emphasize the importance of VS in maintaining hydraulic safety in VS species. Furthermore, the high mortality rate and fast regeneration in NS species may be another hydraulic strategy in regions where severe seasonal droughts are frequent.

Keywords: drought-induced mortality; vulnerability segmentation; seasonal drought; hydraulic conductivity; sapwood density

1. Introduction

In the context of climate change, longer and more intense droughts have been projected [1], and widespread vegetation mortality will be induced by ongoing drought events [2,3], which may drive rapid shifts of vegetation structure and species composition [4,5]. During droughts, the long-distance water transport pathway may be impaired by air-seeded embolisms in xylem conduits [6–8]. Prolonged drought may induce hydraulic failure, which is related to canopy dieback, and even widespread plant mortality [9–11].

Plants employ a range of adaptive strategies to maintain hydraulic safety during drought events. During a midday water deficit, stomatal control regulates leaf transpiration and maintains the diurnal integrity of the water transport pathway [12,13]. In general, leaves are more vulnerable to drought-induced embolism than stems due to positive differences in the water potential at 50% loss

of hydraulic conductance between leaves and terminal stems ($P_{50\text{leaf-stem}}$), which shows hydraulic vulnerability segmentation (VS) [14,15]. Leaves may act as a “safety valve” to protect stems and trunks from hydraulic failure during drought events. Plants tend to sacrifice the phenotypically plastic leaves and maintain carbon-cost branches and trunks [16]. In addition, leaf shedding may prevent catastrophic hydraulic failure and maintain hydraulic safety in stems during seasonal droughts [7,17–20]. However, some tree species have been indicated to lack vulnerability segmentation (NS species), not only in humid tropical and subtropical forests [21,22], but also in arid savanna ecosystems [20] and in temperate mixed forests [23]. NS species have been found in both deciduous and evergreen woody species [24–30], while a few have also shown that herbaceous species were also non-segmented species [31]. These NS species may exhibit compensatory hydraulic strategies to cope with drought stress such as leaf shedding, deep roots, greater xylem hydraulic conductivity, and greater water storage in sapwood [22,23,32,33].

The river valleys in Southwest China host a dry-hot climate with strong seasonality of precipitation [34]. The seasonal drought from November to April puts selective pressure on divergent hydraulic strategies across species differing in leaf habits [20]. Our previous research suggested that drought-deciduous species in the Chinese savanna lacks VS and sheds leaves at the expense of top shoots during peak drought. Otherwise, evergreen and winter-deciduous tree species displayed a coordination of VS and strong stomatal regulation to cope with seasonal drought [20]. Given the impact of hydraulic strategies on the growth and survival of plant species, drought-induced hydraulic dysfunction may cause canopy dieback, and even whole plant mortality [10,32]. To our knowledge, there is still a lack of information about the difference in drought-induced mortality regarding VS and NS species.

In this study, we surveyed the mortality and recruitment rate, the hydraulic traits of leaf and stem, and the photosynthesis of co-occurring tree species in a savanna ecosystem in Southwest China. By analyzing the relationships between tree mortality and hydraulic traits, the main objective of this study was to test whether hydraulic VS was related to drought-induced mortality. Based on the VS paradigm, VS is crucial to survive droughts [16]. In addition, the capacity of plants to resist embolism formation can indicate their drought tolerance and chances of survival [29]. Specifically, we tested whether tree mortality and recruitment rates differed between VS species and NS species. We hypothesized that VS species have low drought-induced mortality, but NS species exhibited robust cavitation-resistant leaves and a negative $P_{50\text{leaf-stem}}$, thus, lacked a “safety valve” to protect the stems and trunks from hydraulic failure during drought events. This risky hydraulic strategy may lead to a high drought-induced mortality rate during seasonal drought, however, NS species may have high hydraulic conductivity and photosynthetic carbon gain, which promotes rapid growth and regeneration under suitable growth conditions.

2. Materials and Methods

2.1. Study Site

This study was carried out at the Yuanjiang Savanna Ecosystem Research Station (23°27' N, 102°10' E, and 481 m above sea level), Yuanjiang County, Yunnan Province, Southwest China. The study site hosts a valley-type savanna [34]. The dominant tree species are *Lannea coromandelica*, *Polyalthia cerasoides*, *Woodfordia fruticosa*, and *Bauhinia brachycarpa*. The climate has a distinct seasonality: rainy season (May–October) and dry season (November–April). According to the meteorological data at this station (2012–2017), the mean annual temperature is 24.7 °C, and the mean annual total precipitation is 732.8 mm; however, approximately 80% of the precipitation occurs during the rainy season. The soil water content then decreases sharply from November to April, which indicates a seasonal drought of six months (Figure S1).

2.2. Plant Materials

At the end of 2011, a 1 ha (100 × 100 m) long-term plot was built for a savanna ecosystem. This plot was divided into 100 subplots of 10 × 10 m. All individuals with a diameter in breast height (DBH) of ≥1 cm were identified, measured, and mapped in the middle of the rainy season (July–August) of 2012. There were 23 tree species in this plot. In order to avoid the randomness of tree growth and mortality caused by small samples ($n < 50$), we selected six tree species with more than 50 individuals per species: *Bauhinia brachycarpa* (Bb, Leguminosae Family), *Woodfordia fruticosa* (Wf, Lythraceae Family), *Campylotropis delavayi* (Cd, Leguminosae Family), *Polyalthia cerasoides* (Pc, Annonaceae Family), *Lannea coromandelica* (Lc, Ebenaceae Family), and *Diospyros yunnanensis* (Dy, Ebenaceae Family) (Table S1). The mortality and recruitment were re-surveyed in the middle of the rainy season of 2017. Both plot surveys were carried out during the plant growth seasons. Plants were recorded as dead if no leaves or living buds and dried inner bark and cambium were observed [5,35]. Many factors may contribute to tree mortality such as drought, heat stress, and insect attacks [36]. However, there was neither insect outbreak nor heat wave in this region during 2012–2017, thus, the tree mortality was attributed to seasonal drought. The mortality rate (MR, %) and recruitment rate (RR, %) were determined as follows [37]:

$$MR = (\ln N_0 - \ln St)/T \quad (1)$$

$$RR = (\ln Nt - \ln St)/T \quad (2)$$

where N_0 is the number of living individuals in 2012; Nt is the number of living individuals in 2017; and St is the number of living individuals in both 2012 and 2017. In this study, the survey interval was five year, thus, $T = 5$.

The abbreviation of functional traits is in Table 1.

Table 1. The functional traits, their abbreviations, and units in this study.

Functional Traits	Abbreviation	Unit
Mortality rate	MR	%
Recruitment rate	RR	%
Xylem tension at 50% loss of stem hydraulic conductivity	$P_{50\text{stem}}$	MPa
Leaf water potential at 50% loss of leaf hydraulic conductance	$P_{50\text{leaf}}$	MPa
Water potential difference at 50% loss of hydraulic conductance between leaves terminal stems	$P_{50\text{leaf-stem}}$	MPa
Sapwood-specific hydraulic conductivity	K_S	$\text{kg m}^{-1} \text{s}^{-1} \text{MPa}^{-1}$
Leaf-specific hydraulic conductivity	K_L	$10^{-4} \text{kg m}^{-1} \text{s}^{-1} \text{MPa}^{-1}$
Cross sapwood area per distal leaf area, Huber value	HV	$\text{mm}^2 \text{m}^{-2}$
Leaf mass per area	LMA	g m^{-2}
Sapwood density	ρ_{sapwood}	g cm^{-3}
Maximum net photosynthetic rate based on leaf area	A_{max}	$\mu\text{mol m}^{-2} \text{s}^{-1}$
Stomatal conductance	g_s	$\text{mol m}^{-2} \text{s}^{-1}$

2.3. Vulnerability Curves of Leaf and Stem

Terminal branches with fully sun-exposed and healthy leaves from the upper canopy were used to determine the hydraulic traits of the leaves and stems. During the 2014 rainy season (July–August), five terminal branches were sampled from 3–5 individuals per species for predawn analysis. The branch cut ends were sealed with moist towels and transported in a sampling box to the laboratory as soon as possible. The leaf water potential (ψ_{pd}) of sampled leaves were measured and summarized in Table S2.

Leaf vulnerability curves were determined according to the method described by Franks (2006) [38]. Healthy, mature leaves were submerged in water to rehydrate, then leaves were placed on a laboratory bench to obtain different leaf water potentials. Initial leaf water potential (Ψ_1) was measured using a pressure chamber (PMS, Corvallis, OR, USA), allowed to equilibrate for 2 min, and then the pressure

was increased to a higher value (Ψ_2). We collected the extruded xylem sap from petioles within 10 s and measured its sap mass (SM). The leaf area (LA) was determined with a Li-3000A leaf area meter (Li-Cor, Lincoln, NE, USA). K_{leaf} was determined as follows

$$K_{\text{leaf}} = \frac{SM}{10 * M * (\psi_2 - \psi_1) * LA} \quad (3)$$

where the parameter M is the molar mass of water (18 g mol^{-1}). The relationships between K_{leaf} and Ψ_{leaf} were fitted to a sigmoidal curve (Figure S2), and the leaf water potential at 50% loss of K_{leaf} ($P_{50\text{leaf}}$) was derived from the fitted equation.

The air injection method was used to measure stem vulnerability curves [39]. First, the maximum vessel length (MVL) for each species was determined using the air injection method [40]. Then, stem segments longer than the MVL were used to determine stem hydraulic conductivity (Table S2), which may avoid an open-vessel artefact [41]. We re-cut the stem ends under distilled water and shaved them with a sharp razor blade. A pressure of 0.1 MPa was used to flush the stems with potassium chloride solution (KCl) for at least 20 min to remove air embolisms. Stem hydraulic conductivity was measured using the method described by Sperry and Tyree (1988) [42]. An elevated water pressure was used to drive the flushing solution (0.1 mol L^{-1} KCl solution) through the segments. Hydraulic conductivity per unit pressure gradient (K_h , $\text{kg m s}^{-1} \text{ MPa}^{-1}$) is equal to the ratio between the water flux through an excised stem segment and the pressure gradient causing the flow. Afterward, the sapwood of the segment was flushed with a methyl blue solution and the cross-sapwood area (A_S , mm^2) was calculated as the mean value of the cross section of the two ends of the stem segment. Total distal leaf area (A_L , m^2) for every terminal stem was determined, and the dry mass (DW) of the leaves was determined after drying at 70°C for 48 h. Leaf mass per area (LMA, g cm^{-2}) was calculated as DW/A_L . The Huber value (HV , $\text{mm}^2 \text{ m}^{-2}$) was calculated as A_S/A_L . Sapwood-specific hydraulic conductivity (K_S , $\text{kg m}^{-1} \text{ s}^{-1} \text{ MPa}^{-1}$) was calculated as K_h/A_S . Specific leaf hydraulic conductivity (K_L , $\text{kg m}^{-1} \text{ s}^{-1} \text{ MPa}^{-1}$) was calculated as K_h/A_S .

The above segments were inserted into a pressure chamber (PMS, Corvallis, OR, USA) with both ends protruding. Cavitation was successively induced by this chamber, and hydraulic conductivity was re-measured after equilibrating the segments. This process was repeated until higher than 80% of the maximum K_S was lost. A vulnerability curve was fitted by a sigmoidal function [43].

$$PLC = \frac{100}{1 + \exp[a(P - b)]} \quad (4)$$

where PLC (%) is the percentage loss in stem hydraulic conductivity; P is the xylem water potential; and the parameters a and b are the maximum slope of the curve and xylem water potential at 50% loss of hydraulic conductivity ($P_{50\text{stem}}$), respectively (Figure S3).

2.4. Vulnerability Segmentation

The difference in water potential at 50% loss of hydraulic conductance between leaves and stems ($P_{50\text{leaf-stem}}$) was quantified. Positive and negative values of $P_{50\text{leaf-stem}}$ indicated VS and NS species, respectively [44].

2.5. Sapwood Density

The segments used for hydraulic conductivity measurement were used to measure the sapwood density (ρ_{sapwood} , g cm^{-3}). After removing the bark and pith, the volume of the fresh sapwood (V_{sapwood}) was measured using the water displacement method. The sapwood samples were dried in an oven at 70°C for 72 h and then the dry mass (DW) was determined with a balance ($\pm 0.0001 \text{ g}$). The ρ_{sapwood} was calculated as DW/V_{sapwood} .

2.6. Leaf Gas Exchange Measurements

In the middle of the rainy season, leaf gas exchange was measured from six sun-exposed leaves of three trees per species using a portable photosynthesis system (LI-6400XT, Li-Cor, Lincoln, NE, USA) between 9:00–11:00 on sunny days. The maximum net photosynthetic rate (A_{\max}) and stomatal conductance based on leaf area (g_s) were determined under a CO_2 concentration of $400 \mu\text{mol m}^{-2} \text{s}^{-1}$ and ambient air temperature of $25\text{--}30^\circ\text{C}$. The photosynthetic photon flux density was set to $1200 \mu\text{mol m}^{-2} \text{s}^{-1}$.

2.7. Statistical Analyses

Statistical analyses were performed using the SPSS version 16.0 software package (SPSS, Chicago, IL, USA). The relationships between the traits were analyzed using cross-species Pearson correlations. The differences in tree mortality rate, and the hydraulic and photosynthetic traits between NS species and VS species groups were assessed using independent sample t -tests. Moreover, a principal component analysis (PCA) was performed across traits and species. The significance level was set to $\alpha = 0.05$.

3. Results

3.1. Hydraulic and Photosynthetic Traits

Six tree species showed great variation in hydraulic vulnerability, namely, the values of $P_{50\text{stem}}$ and $P_{50\text{leaf}}$ ranged from $-3.44\text{--}1.74$ MPa, and $-3.71\text{--}1.05$ MPa, respectively (Figure 1a,b). Linking the values of $P_{50\text{stem}}$ and $P_{50\text{leaf}}$ for each species, negative values of $P_{50\text{leaf-stem}}$ were observed for *B. brachycarpa* (-1.02 MPa), *W. fruticosa* (-0.54 MPa), and *C. delavayi* (-0.83 MPa), which indicates that these tree species lacked vulnerability segmentation (NS species). In contrast, positive values of $P_{50\text{leaf-stem}}$ were found for *P. cerasoides* (1.21 MPa), *L. coromandelica* (0.69 MPa), and *D. yunnanensis* (0.76 MPa), which indicates that these tree species had vulnerability segmentation (VS species) between the leaf and stem (Figure 1c). On average, NS species had a significantly lower $P_{50\text{leaf}}$ and $P_{50\text{leaf-stem}}$ than the VS species ($P < 0.05$, Table 2), however, $P_{50\text{stem}}$ did not differ significantly between the NS species and VS species ($P > 0.05$, Table 2). In comparison to VS species, NS species had significantly higher values of HV , A_{\max} , and g_s ($P < 0.05$, Table 2). Values of K_s , K_L , ρ_{sapwood} , and LMA were not significantly different between the NS species and VS species.

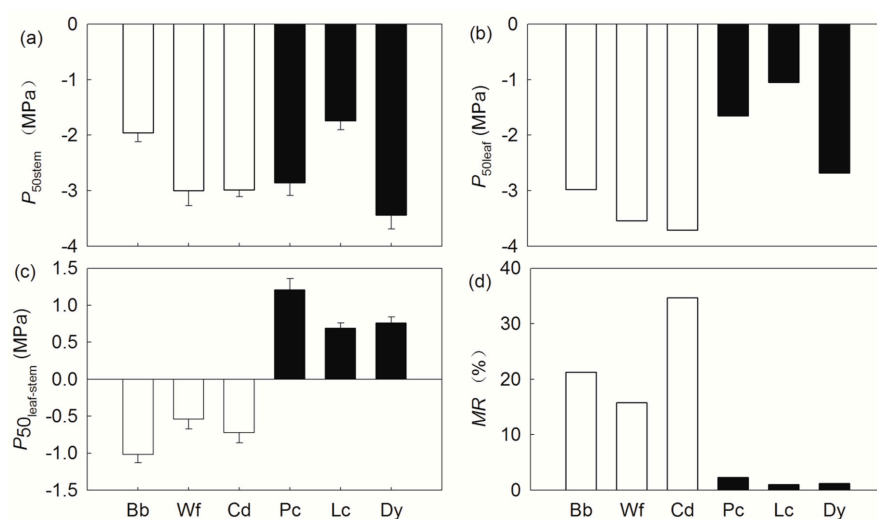


Figure 1. Hydraulic traits and mortality rate in six tree species. The abbreviation of functional traits is in Table 1. (a) $P_{50\text{stem}}$; (b) $P_{50\text{leaf}}$; (c) $P_{50\text{leaf-stem}}$; (d) MR. The hollow and solid bars indicated the NS species and VS species, respectively. The codes of species: *Bauhinia brachycarpa* (Bb), *Woodfordia fruticosa* (Wf), *Campylotropis delavayi* (Cd), *Polyalthia cerasoides* (Pc), *Lannea coromandelica* (Lc), *Diospyros yunnanensis* (Dy).

Table 2. Comparison of the mortality rate, recruitment rate, hydraulic, and photosynthetic traits between NS species and VS species. The abbreviations of the functional traits are shown in Table 1. Significant differences between the NS species and VS species relationships are shown in bold and underlined.

Functional Traits	NS Species	VS Species	T	P Value
MR	23.9 ± 5.6%	1.5 ± 0.01%	8.156	<u>0.001</u>
RR	21.3 ± 7.7%	2.5 ± 0.01%	4.094	<u>0.015</u>
$P_{50\text{stem}}$	−2.65 ± 0.34	−2.68 ± 0.50	0.049	0.963
$P_{50\text{leaf}}$	−3.41 ± 0.28	−1.79 ± 0.48	3.082	<u>0.037</u>
$P_{50\text{leaf-stem}}$	−0.83 ± 0.09	0.89 ± 0.16	7.666	<u>0.002</u>
K_s	3.27 ± 0.59	3.97 ± 1.68	0.394	0.714
K_L	7.79 ± 1.57	4.26 ± 2.41	1.224	0.288
HV	2.36 ± 0.10	1.05 ± 0.22	5.426	<u>0.006</u>
ρ_{sapwood}	0.62 ± 0.03	0.48 ± 0.08	1.671	0.170
LMA	110.60 ± 6.30	82.57 ± 13.97	1.829	0.141
A_{max}	19.3 ± 1.10	11.3 ± 2.19	3.230	<u>0.032</u>
g_s	0.39 ± 0.05	0.17 ± 0.04	3.722	<u>0.020</u>

3.2. Tree Mortality and Recruitment Rate

According to the plot surveys over a five year interval (2012–2017), the six tree species displayed great variation in MR and RR: 34.7-fold (1.0–34.7%) and RR 27-fold (1.3–35.5%), respectively (Figure 1d; Table S1). Compared with VS species, NS species had significantly higher MR and RR ($P < 0.05$, Table 2). In addition, MR was significantly associated with RR across species ($P < 0.05$, Table 3), which indicates that tree mortality was covaried with recruitment across the six savanna tree species studied.

Table 3. Coefficients of the Pearson's correlations between mortality rate, recruitment rate, and hydraulic traits. The abbreviation of functional traits in Table 1. Significant relationships are shown in bold and underlined in the cross-species Pearson's correlation ($P < 0.05$).

Traits	MR	RR	$P_{50\text{stem}}$	$P_{50\text{leaf}}$	$P_{50\text{leaf-stem}}$	K_s	K_L	HV	ρ_{sapwood}	LMA	A_{max}
RR	<u>0.969</u>										
$P_{50\text{stem}}$	−0.047	−0.076									
$P_{50\text{leaf}}$	<u>−0.833</u>	<u>−0.890</u>	0.490								
$P_{50\text{leaf-stem}}$	<u>−0.912</u>	<u>−0.879</u>	−0.158	0.783							
K_s	−0.255	−0.356	0.626	0.578	0.209						
K_L	0.367	0.180	0.388	−0.198	−0.501	0.664					
HV	<u>0.857</u>	0.740	0.018	<u>−0.826</u>	<u>−0.949</u>	−0.123	0.639				
ρ_{sapwood}	0.710	0.741	−0.539	<u>−0.874</u>	−0.605	<u>−0.847</u>	−0.261	0.544			
LMA	0.518	0.425	−0.547	<u>−0.917</u>	−0.648	−0.592	0.168	0.723	0.738		
A_{max}	<u>0.865</u>	0.664	0.272	−0.539	<u>−0.804</u>	0.310	<u>0.825</u>	<u>0.851</u>	0.227	0.326	
g_s	0.628	0.451	0.375	−0.554	<u>−0.895</u>	0.116	0.696	<u>0.839</u>	0.272	0.495	<u>0.818</u>

3.3. Relationship between Tree Performance and Functional Traits

Across the six tree species, MR was significantly associated with $P_{50\text{leaf}}$, $P_{50\text{leaf-stem}}$, and HV ($p < 0.05$, Figure 2b–d), but was not significantly associated with $P_{50\text{stem}}$ ($p > 0.05$, Figure 2a). Meanwhile, RR was also significantly associated with $P_{50\text{leaf}}$ and $P_{50\text{leaf-stem}}$ ($p < 0.05$, Table 3). $P_{50\text{leaf}}$ was significantly associated with ρ_{sapwood} and LMA ($p < 0.05$, Table 3). The association of $P_{50\text{stem}}$ and K_s was not significant ($p > 0.05$, Table 3), which indicates that there was no trade-off between hydraulic safety and efficiency.

Given the relationships between hydraulic efficiency and photosynthesis, A_{max} was significantly associated with K_L and HV, and a significant association between A_{max} and g_s was found across all six species ($p < 0.05$, Table 3). In addition, there was a negatively significant association between K_s and ρ_{sapwood} ($p < 0.05$, Table 3).

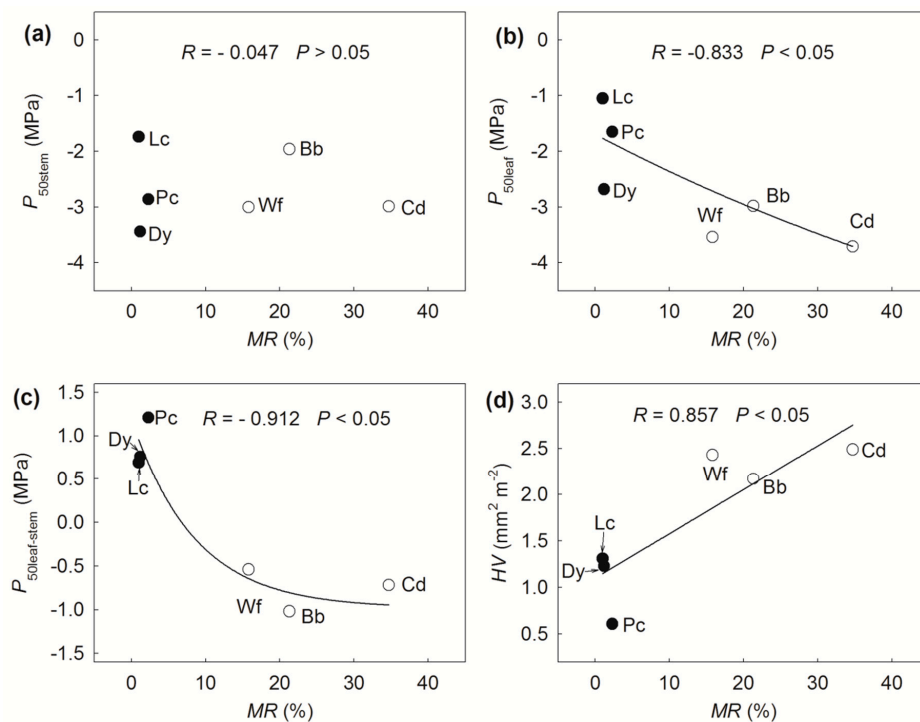


Figure 2. Relationships between mortality rate and hydraulic traits in the six tree species. The abbreviation of functional traits and species codes as shown in Table 1 and Figure 1, respectively. (a) P_{50stem} and MR; (b) P_{50leaf} and MR; (c) $P_{50leaf-stem}$ and MR; (d) HV and MR. The hollow and solid circles indicate the NS species and VS species, respectively.

3.4. Principal Component Analysis (PCA)

PCA was used to evaluate how tree performance and functional traits were associated by pooling data across species (Figure 3). The first axis of the PCA explained 57.6% of the total variation in traits and tree performance, which was associated with MR, RR, HV, LMA, $P_{50leaf-stem}$, and P_{50leaf} (Figure 3a). The second axis of the PCA explained 28.7% of the total variations, along with K_s , P_{50stem} , and K_l (Figure 3a). PCA analysis for the six tree species indicated that NS species tend to have more negative $P_{50leaf-stem}$, higher HV values, and higher MR and RR. In contrast, VS species tended to have more positive $P_{50leaf-stem}$ and lower MR and RR (Figure 3b).

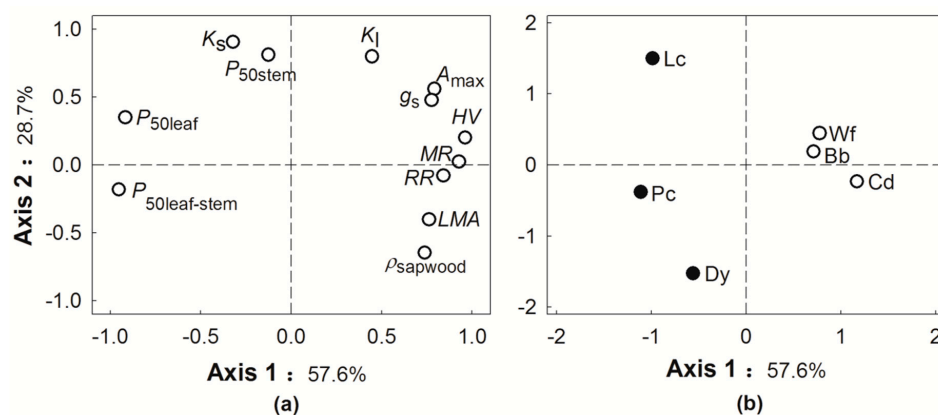


Figure 3. Principal component analysis (PCA) for twelve functional traits (a) and six tree species (b). The abbreviation of functional traits and species codes are shown in Table 1 and Figure 1, respectively. The hollow and solid circles in Figure 3b indicate the NS species and VS tree species, respectively.

4. Discussion

In this study, the NS species displayed a higher *MR* compared with the VS species (Table 2). This result was consistent with our hypothesis, namely, that VS species have lower drought-induced mortality rates, but NS species adopt risky hydraulic strategies and suffer from higher drought-induced mortality during prolonged seasonal drought. Additionally, *MR* was significantly associated with $P_{50\text{leaf-stem}}$ and $P_{50\text{leaf}}$ across species (Figure 2b,c). These results demonstrated that VS plays a crucial role in drought avoidance or tolerance in VS species; in contrast, NS species with higher *MR* displayed a higher *RR* compared with VS species, which was associated with photosynthesis (Figure 3; Table 3).

4.1. Tree Mortality Was Related to Vulnerability Segmentation

Our site has a distinct seasonality of precipitation, with a total annual precipitation of 732.8 mm, but only 20% falls from November to April (Figure S1). The soil water content decreased sharply from November and dropped to below 10% by the end of the dry season (March) (Figure S1). A seasonal drought of six months has been suggested to put a selective pressure on the differentiation of hydraulic and growth strategies [20]. Our results suggested that VS plays a crucial role in drought avoidance or tolerance in VS species, in contrast, NS species with high mortality rates and fast regeneration, adopt risky hydraulic safety strategies and exhibit high hydraulic conductivity and photosynthesis rates. To our knowledge, this study is the first to identify the difference in drought-induced tree mortality between NS and VS species.

In this study, *MR* was significantly associated with $P_{50\text{leaf-stem}}$ and $P_{50\text{leaf}}$, but not associated with $P_{50\text{stem}}$ across species (Figure 2a–c). This result is somewhat inconsistent with previous results obtained with subtropical tree saplings [45] and insular pines [46]. We emphasized the importance of VS in tree mortality, which indicated the distinct hydraulic strategies between VS and NS species. Three VS species exhibited positive $P_{50\text{leaf-stem}}$ values (Figure 1c), accordingly, their leaves were more vulnerable to drought-induced cavitation than the stems. VS species generally displayed more conservative hydraulic strategies such as strong stomatal regulation and leaf shedding at the beginning of drought [13,20]. More vulnerable leaves may act as “safety valves” to protect the hydraulic safety of stems and trunks under midday or seasonal drought [13,15,26]. With respect to “safety valves” of more vulnerable leaves, we concluded that hydraulic VS between leaves and distal branches play an important role in hydraulic safety and survival under prolonged seasonal drought. The VS species *L. coromandelica* exhibited strong stomatal regulation and sacrificed the “cheaper” and more vulnerable leaves to maintain the hydraulic safety of the more carbon-costly stems from the beginning of seasonal drought [20]. This result supported the role of hydraulic VS in maintaining hydraulic safety for VS species. On the other hand, NS species have been suggested to exhibit risky hydraulic strategies as they lack “safety valve” roles and obvious stomatal regulation from embolism-resistant leaves [22,33,47]. When NS species were exposed to severe or prolonged drought, persistent excess water demand due to evaporation and transpiration exceeded the water supply [36], which subsequently resulted in catastrophic hydraulic failure when excess embolism via air seeding occurred in the xylem [5,8,11]. *Terminthia paniculata*, one of the NS species in this savanna, shed leaves until peak drought after sacrificing some top shoots and all of the leaves attached to these branches [20]. We speculated that high *MR* in three NS species resulted from the catastrophic hydraulic failure during a long seasonal drought.

No significant association between *MR* and ρ_{sapwood} was found in our study (Table 3) and our results were not consistent with the strong tendency that tree species with low wood density are at greater risk of drought-induced mortality [48]. Two explanations for the inconsistent results are suggested. First, it is suggested that species with dense wood may exhibit large declines in water potential, and therefore, are subject to more extensive embolism in the xylem, and low hydraulic safety. In contrast, species with low wood density display strong stomatal regulation and maintain a high leaf water potential [5]. Second, wood density may not be an indicator of tree growth and survival [45,49]. Wood is a complex component of the vessels, fiber area, and parenchyma cells [49,50], and in addition

to water transport, wood also provides mechanical strength [51,52]. Plants may develop wood traits for comprehensive adaptation to a selective pressure.

$P_{50\text{leaf}}$ in the NS species was significantly more negative than in the VS species. Moreover, $P_{50\text{leaf}}$ was significantly associated with LMA ($P < 0.05$, Table 3). Our results indicate that NS species develop more embolism-resistant leaves than VS species. A lower specific leaf area (higher LMA) indicated a higher resistance to drought [48,53]. A higher LMA can keep the stomata open and promote photosynthesis during mild and moderate drought [23]. However, NS species lack “safety valves” and obvious stomatal regulation from embolism-resistant leaves, which induces excess embolism in xylem [33,47]. Under a long seasonal drought, a risky hydraulic strategy results in the catastrophic hydraulic failure of more vulnerable stems and trunks, and even tree mortality.

4.2. Hydraulic Traits and Photosynthesis

It is widely noted that efficient water supply in leaves is closely associated with photosynthesis and growth [40,54–56]. The specific hydraulic conductivity in sapwood was not higher in the NS species than in the VS Species (Table 2; Table S2). The NS species made architectural adjustments to increase sapwood area per unit leaf area (higher HV), which improves stem water transport capacity to the distal leaves [57,58].

Under optimal conditions, higher K_L allows the leaves to maintain higher leaf water potential and g_s , and subsequently maintain greater photosynthesis rates [54,56,59]. In this study, K_L was significantly positively correlated with A_{max} (Table 3), representing a coordination of hydraulics and photosynthesis, which is consistent with previous results [40,54]. NS species tend to adopt risky water-use efficiency and maintain a higher photosynthetic carbon gain [22,23,47]. In the dry–hot valleys, even during the middle of the rainy season, when soil water is abundant, the midday air temperature is 28–35 °C (Figure S1) and the leaf-to-air vapor pressure deficit (VPD) is 1.5–2.5 Kpa in the morning, however, the VPD can reach more than 3.5 kPa at noon, even during the rainy season (data not shown). Previous studies have suggested that high VPD significantly affects stomatal behavior and photosynthetic water use efficiency [40]. Higher photosynthetic carbon gain also promotes rapid growth during rainy seasons. To a large extent, higher RR in NS species can be attributed to a higher capacity of photosynthetic carbon uptake. However, RR are also related to flower and seed production and fecundity of the plants [60]. Further studies are needed to test the associations of plant recruitment, hydraulic traits, and reproductive strategies.

5. Conclusions and Implications

Based on a comparable study of tree performance and hydraulic traits, we found evidence that VS plays a crucial role in drought avoidance or tolerance in VS species. In contrast, NS species have high mortality rates and fast regeneration, adopts risky hydraulic safety strategies, and exhibit a high photosynthesis rate. The present study emphasized the importance of VS in maintaining hydraulic safety for VS species. Furthermore, high mortality and fast regeneration in NS species may be another hydraulic strategy in regions where prolonged seasonal drought is frequent. Although NS species have fast regeneration in the dry–rainy season cycles, three of the NS species in this study were small trees or shrubs (Table S1). It has been suggested that most forest trees are at risk of drought-induced mortality due to narrow hydraulic safety margins [8]. In future, more extensive, severe, or frequent drought may induce global forest dieback [2] and substantial tree mortality may become a consequence of the extreme droughts under global climate change [61]. Moreover, larger trees may be at a larger risk of drought-induced mortality [62]. In the dry–wet cycles, both NS species and VS tree species may face mortality during droughts, and recruit in suitable growth conditions. However, NS species may display an advantage of regeneration over VS species under dry–wet circles. This regeneration may promote the growth of more small trees and shrubs during extreme drought events, with an obvious decline in biomass and ecosystem carbon storage in seasonal forests.

Supplementary Materials: The following are available online at <http://www.mdpi.com/1999-4907/10/8/697/s1>, Table S1: Characteristics of tree species included in this study, Table S2: Hydraulic and photosynthetic traits of the tree species in this study, Table S3: Factor loading, eigenvalues, the percentage of functional traits explained by the first two principal components, Figure S1: The monthly air temperature, monthly precipitation and soil water content in our study from 2012–2017, Figure S2: Leaf vulnerability curves for the six tree species in this study, Figure S3: Stem vulnerability curves for the six tree species in this study.

Author Contributions: S.Z., G.W., and D.Y. collected the experimental data. S.Z. analyzed the data and wrote the manuscript.

Funding: This study was funded by the National Natural Science Foundation of China (31600479; 31870385; 41861144016), the CAS Scholarship for visiting research (No. 2018-24), and the CAS “Light of West China” Program to Shubin Zhang.

Acknowledgments: We are very grateful to the Yuanjiang Savanna Ecosystem Research Station, Xishuangbanna Tropical Botanical Garden, Chinese Academy of Sciences for providing climate data and the tree surveys. We also thank Wanyou Dao for sampling assistance in the field.

Conflicts of Interest: The authors declare there are no conflict of interest.

References

1. Trenberth, K.E.; Dai, A.; van der Schrier, G.; Jones, P.D.; Barichivich, J.; Briffa, K.R.; Sheffield, J. Global warming and changes in drought. *Nat. Clim. Chang.* **2014**, *4*, 17–22. [[CrossRef](#)]
2. Allen, C.D.; Macalady, A.K.; Chenchouni, H.; Bachelet, D.; McDowell, N.; Vennetier, M.; Kitzberger, T.; Rigling, A.; Breshears, D.D.; Hogg, E.; et al. A global overview of drought and heat-induced tree mortality reveals emerging climate change risks for forests. *For. Ecol. Manag.* **2010**, *259*, 660–684. [[CrossRef](#)]
3. Martínez-Vilalta, J.; Lloret, F. Drought-induced vegetation shifts in terrestrial ecosystems: The key role of regeneration dynamics. *Glob. Planet. Chang.* **2016**, *144*, 94–108. [[CrossRef](#)]
4. Allen, C.D.; Breshears, D.D. Drought-induced shift of a forest-woodland ecotone: Rapid landscape response to climate variation. *Proc. Natl. Acad. Sci. USA* **1998**, *95*, 14839–14842. [[CrossRef](#)] [[PubMed](#)]
5. Hoffmann, W.A.; Marchin, R.M.; Abit, P.; Lau, O.L. Hydraulic failure and tree dieback are associated with high wood density in a temperate forest under extreme drought. *Glob. Chang. Boil.* **2011**, *17*, 2731–2742. [[CrossRef](#)]
6. Hacke, U.G.; Sperry, J.S.; Pittermann, J. Drought experience and cavitation resistance in six shrubs from the Great Basin, Utah. *Basic Appl. Ecol.* **2000**, *1*, 31–41. [[CrossRef](#)]
7. Choat, B.; Ball, M.C.; Luly, J.G.; Holtum, J.A.M. Hydraulic architecture of deciduous and evergreen dry rainforest tree species from north-eastern Australia. *Trees-Struct. Funct.* **2005**, *19*, 305–311. [[CrossRef](#)]
8. Choat, B.; Jansen, S.; Brodribb, T.J.; Cochard, H.; Delzon, S.; Bhaskar, R.; Bucci, S.J.; Feild, T.S.; Gleason, S.M.; Hacke, U.G.; et al. Global convergence in the vulnerability of forests to drought. *Nature* **2012**, *491*, 752–755. [[CrossRef](#)]
9. Davis, S.D.; Ewers, F.W.; Sperry, J.S.; Portwood, K.A.; Crocker, M.C.; Adams, G.C. Shoot dieback during prolonged drought in Ceanothus (Rhamnaceae) chaparral of California: A possible case of hydraulic failure. *Am. J. Bot.* **2002**, *89*, 820–828. [[CrossRef](#)]
10. Anderegg, W.R.L.; Berry, J.A.; Smith, D.D.; Sperry, J.S.; Anderegg, L.D.L.; Field, C.B. The roles of hydraulic and carbon stress in a widespread climate-induced forest die-off. *Proc. Natl. Acad. Sci. USA* **2012**, *109*, 233–237. [[CrossRef](#)]
11. Choat, B.; Brodribb, T.J.; Brodersen, C.R.; Duursma, R.A.; López, R.; Medlyn, B.E. Triggers of tree mortality under drought. *Nature* **2018**, *558*, 531–539. [[CrossRef](#)] [[PubMed](#)]
12. Zhang, Y.J.; Meinzer, F.C.; Qi, J.H.; Goldstein, G.; Cao, K.F. Midday stomatal conductance is more related to stem rather than leaf water status in subtropical deciduous and evergreen broadleaf trees. *Plant Cell Environ.* **2013**, *36*, 149–158. [[CrossRef](#)] [[PubMed](#)]
13. Liu, Y.-Y.; Song, J.; Wang, M.; Li, N.; Niu, C.-Y.; Hao, G.-Y. Coordination of xylem hydraulics and stomatal regulation in keeping the integrity of xylem water transport in shoots of two compound-leaved tree species. *Tree Physiol.* **2015**, *35*, 1333–1342. [[CrossRef](#)] [[PubMed](#)]
14. Zimmermann, M.H. *Xylem Structure and the Ascent of Sap*; Springer: Berlin, Germany, 1983.
15. Tyree, M.T.; Cochard, H.; Cruiziat, P.; Sinclair, B.; Ameglio, T. Drought-induced leaf shedding in walnut: Evidence for vulnerability segmentation. *Plant Cell Environ.* **1993**, *16*, 879–882. [[CrossRef](#)]

16. Johnson, D.M.; Wortemann, R.; McCulloh, K.A.; Jordan-Meille, L.; Ward, E.; Warren, J.M.; Palmroth, S.; Domec, J.-C. A test of the hydraulic vulnerability segmentation hypothesis in angiosperm and conifer tree species. *Tree Physiol.* **2016**, *36*, 983–993. [[CrossRef](#)] [[PubMed](#)]
17. Wolfe, B.T.; Sperry, J.S.; Kursar, T.A. Does leaf shedding protect stems from cavitation during seasonal droughts? A test of the hydraulic fuse hypothesis. *New Phytol.* **2016**, *212*, 1007–1018. [[CrossRef](#)] [[PubMed](#)]
18. Ambrose, A.R.; Baxter, W.L.; Martin, R.E.; Francis, E.; Asner, G.P.; Nydick, K.R.; Dawson, T.E. Leaf- and crown-level adjustments help giant sequoias maintain favorable water status during severe drought. *For. Ecol. Manag.* **2018**, *419–420*, 257–267. [[CrossRef](#)]
19. Jump, A.S.; Ruiz-Benito, P.; Greenwood, S.; Allen, C.D.; Kitzberger, T.; Fensham, R.; Lloret, F.; Ruiz-Benito, P.; Martínez-Vilalta, J.; Ruiz-Benito, P.; et al. Structural overshoot of tree growth with climate variability and the global spectrum of drought-induced forest dieback. *Glob. Chang. Biol.* **2017**, *23*, 3742–3757. [[CrossRef](#)]
20. Zhang, S.-B.; Zhang, J.-L.; Cao, K.-F. Divergent Hydraulic Safety Strategies in Three Co-occurring Anacardiaceae Tree Species in a Chinese Savanna. *Front. Plant Sci.* **2017**, *7*, 504. [[CrossRef](#)]
21. Villagra, M.; Campanello, P.I.; Bucci, S.J.; Goldstein, G. Functional relationships between leaf hydraulics and leaf economic traits in response to nutrient addition in subtropical tree species. *Tree Physiol.* **2013**, *33*, 1308–1318. [[CrossRef](#)]
22. Zhu, S.D.; Liu, H.; Xu, Q.Y.; Cao, K.F.; Ye, Q. Are leaves more vulnerable to cavitation than branches? *Funct. Ecol.* **2016**, *30*, 1740–1744. [[CrossRef](#)]
23. Jin, Y.; Wang, C.K.; Zhou, Z.H. Conifers but not angiosperms exhibit vulnerability segmentation between leaves and branches in a temperate forest. *Tree Physiol.* **2019**, *39*, 454–462. [[CrossRef](#)] [[PubMed](#)]
24. Cochard, H.; Breda, N.; Granier, A.; Aussenac, G. Vulnerability to air embolism of three European species (*Quercus petraea* (Matt) Liebl, *Q. pubescens* Willd, *Q. robur* L). *Ann. For. Sci.* **1992**, *49*, 225–233. [[CrossRef](#)]
25. Choat, B.; Lahr, E.C.; Melcher, P.J.; Zwieniecki, M.A.; Holbrook, N.M. The spatial pattern of air seeding thresholds in mature sugar maple trees. *Plant Cell Environ.* **2005**, *28*, 1082–1089. [[CrossRef](#)]
26. Pivovarovoff, A.L.; Sack, L.; Santiago, L.S. Coordination of stem and leaf hydraulic conductance in southern California shrubs: A test of the hydraulic segmentation hypothesis. *New Phytol.* **2014**, *203*, 842–850. [[CrossRef](#)]
27. Bouche, P.S.; Delzon, S.; Choat, B.; Badel, E.; Brodribb, T.J.; Burlett, R.; Cochard, H.; Charra-Vaskou, K.; Lavigne, B.; Li, S.; et al. Are needles of *Pinus pinaster* more vulnerable to xylem embolism than branches? New insights from X-ray computed tomography. *Plant Cell Environ.* **2015**, *39*, 860–870. [[CrossRef](#)] [[PubMed](#)]
28. Hochberg, U.; Windt, C.W.; Ponomarenko, A.; Zhang, Y.-J.; Gersony, J.; Rockwell, F.E.; Holbrook, N.M. Stomatal Closure, Basal Leaf Embolism, and Shedding Protect the Hydraulic Integrity of Grape Stems. *Plant Physiol.* **2017**, *174*, 764–775. [[CrossRef](#)]
29. Skelton, R.P.; Dawson, T.E.; Thompson, S.E.; Shen, Y.; Weitz, A.P.; Ackerly, D. Low Vulnerability to Xylem Embolism in Leaves and Stems of North American Oaks. *Plant Physiol.* **2018**, *177*, 1066–1077. [[CrossRef](#)]
30. Klepsch, M.; Zhang, Y.; Kotowska, M.M.; Lamarque, L.J.; Nolf, M.; Schuldt, B.; Torres-Ruiz, J.M.; Qin, D.-W.; Choat, B.; Delzon, S.; et al. Is xylem of angiosperm leaves less resistant to embolism than branches? Insights from microCT, hydraulics, and anatomy. *J. Exp. Bot.* **2018**, *69*, 5611–5623. [[CrossRef](#)]
31. Skelton, R.P.; Brodribb, T.J.; Choat, B. Casting light on xylem vulnerability in an herbaceous species reveals a lack of segmentation. *New Phytol.* **2017**, *214*, 561–569. [[CrossRef](#)]
32. McDowell, N.; Pockman, W.T.; Allen, C.D.; Breshears, D.D.; Cobb, N.; Kolb, T.; Plaut, J.; Sperry, J.; West, A.; Williams, D.G.; et al. Mechanisms of plant survival and mortality during drought: Why do some plants survive while others succumb to drought? *New Phytol.* **2010**, *178*, 719–739. [[CrossRef](#)] [[PubMed](#)]
33. Johnson, D.M.; Domec, J.-C.; Woodruff, D.R.; McCulloh, K.A.; Meinzer, F.C. Contrasting hydraulic strategies in two tropical lianas and their host trees. *Am. J. Bot.* **2013**, *100*, 374–383. [[CrossRef](#)] [[PubMed](#)]
34. Jin, Z.Z.; Ou, X.K. *Vegetations in the Hot and Dry Valleys along the Yuanjiang, Nuijiang, Jinshajiang, and Lanchangjiang Rivers*; Yunnan University Press: Kunming, China, 2000.
35. Smith, T.F.; Rizzo, D.M.; North, M. Patterns of mortality in an old-growth mixed-conifer forest of the southern Sierra Nevada, California. *For. Sci.* **2005**, *51*, 266–275.
36. Anderegg, W.R.L.; Hicke, J.A.; Fisher, R.A.; Allen, C.D.; Aukema, J.; Bentz, B.; Hood, S.; Lichstein, J.W.; Macalady, A.K.; McDowell, N.; et al. Tree mortality from drought, insects, and their interactions in a changing climate. *New Phytol.* **2015**, *208*, 674–683. [[CrossRef](#)] [[PubMed](#)]

37. Condit, R.; Ashton, P.S.; Manokaran, N.; LaFrankie, J.V.; Hubbell, S.P.; Foster, R.B. Dynamics of the forest communities at Pasoh and Barro Colorado: Comparing two 50-ha plots. *Philos. Trans. R. Soc. B Boil. Sci.* **1999**, *354*, 1739–1748. [[CrossRef](#)] [[PubMed](#)]
38. Franks, P.J. Higher rates of leaf gas exchange are associated with higher leaf hydrodynamic pressure gradients. *Plant Cell Environ.* **2006**, *29*, 584–592. [[CrossRef](#)] [[PubMed](#)]
39. Cochard, H.; Cruiziat, P.; Tyree, M.T. Use of positive pressures to establish vulnerability curves—Further support for the air-seeding hypothesis and implications for pressure-volume analysis. *Plant Physiol.* **1992**, *100*, 205–209. [[CrossRef](#)] [[PubMed](#)]
40. Brodribb, T.J.; Field, T.S. Stem hydraulic supply is linked to leaf photosynthetic capacity: Evidence from New Caledonian and Tasmanian rainforests. *Plant Cell Environ.* **2000**, *23*, 1381–1388. [[CrossRef](#)]
41. Cochard, H.; Badel, E.; Herbette, S.; Delzon, S.; Choat, B.; Jansen, S. Methods for measuring plant vulnerability to cavitation: A critical review. *J. Exp. Bot.* **2013**, *64*, 4779–4791. [[CrossRef](#)]
42. Sperry, J.S.; Tyree, M.T. Mechanism of Water Stress-Induced Xylem Embolism. *Plant Physiol.* **1988**, *88*, 581–587. [[CrossRef](#)]
43. Van Der Willigen, C.; Pammenter, N.W. A mathematical and statistical analysis of the curves illustrating vulnerability of xylem to cavitation. *Tree Physiol.* **1998**, *18*, 589–593.
44. Johnson, D.M.; McCulloh, K.A.; Woodruff, D.R.; Meinzer, F.C. Hydraulic safety margins and embolism reversal in stems and leaves: Why are conifers and angiosperms so different? *Plant Sci.* **2012**, *195*, 48–53. [[CrossRef](#)] [[PubMed](#)]
45. Zhu, S.-D.; He, P.-C.; Li, R.-H.; Fu, S.-L.; Lin, Y.-B.; Zhou, L.-X.; Cao, K.-F.; Ye, Q. Drought tolerance traits predict survival ratio of native tree species planted in a subtropical degraded hilly area in South China. *For. Ecol. Manag.* **2018**, *418*, 41–46. [[CrossRef](#)]
46. López, R.; De Heredia, U.L.; Collada, C.; Cano, F.J.; Emerson, B.C.; Cochard, H.; Gil, L. Vulnerability to cavitation, hydraulic efficiency, growth and survival in an insular pine (*Pinus canariensis*). *Ann. Bot.* **2013**, *111*, 1167–1179. [[CrossRef](#)] [[PubMed](#)]
47. Bucci, S.J.; Scholz, F.G.; Peschiutta, M.L.; Arias, N.S.; Meinzer, F.C.; Goldstein, G. The stem xylem of Patagonian shrubs operates far from the point of catastrophic dysfunction and is additionally protected from drought-induced embolism by leaves and roots. *Plant Cell Environ.* **2013**, *36*, 2163–2174. [[CrossRef](#)] [[PubMed](#)]
48. Greenwood, S.; Ruiz-Benito, P.; Martínez-Vilalta, J.; Lloret, F.; Kitzberger, T.; Allen, C.D.; Fensham, R.; Laughlin, D.C.; Kattge, J.; Bönsch, G.; et al. Tree mortality across biomes is promoted by drought intensity, lower wood density and higher specific leaf area. *Ecol. Lett.* **2017**, *20*, 539–553. [[CrossRef](#)]
49. Fan, Z.-X.; Zhang, S.-B.; Hao, G.-Y.; Slik, J.F.; Cao, K.-F.; Fan, Z.; Zhang, S.; Hao, G.; Cao, K. Hydraulic conductivity traits predict growth rates and adult stature of 40 Asian tropical tree species better than wood density. *J. Ecol.* **2012**, *100*, 732–741. [[CrossRef](#)]
50. Scholz, F.G.; Bucci, S.J.; Goldstein, G.; Meinzer, F.C.; Franco, A.C.; Miralles-Wilhelm, F. Biophysical properties and functional significance of stem water storage tissues in Neotropical savanna trees. *Plant Cell Environ.* **2007**, *30*, 236–248. [[CrossRef](#)]
51. Niklas, K.J. The mechanical role of bark. *Am. J. Bot.* **1999**, *86*, 465–469. [[CrossRef](#)]
52. Onoda, Y.; Richards, A.E.; Westoby, M. The relationship between stem biomechanics and wood density is modified by rainfall in 32 Australian woody plant species. *New Phytol.* **2010**, *185*, 493–501. [[CrossRef](#)]
53. Poorter, H.; Niinemets, Ü.; Poorter, L.; Wright, I.J.; Villar, R. Causes and consequences of variation in leaf mass per area (LMA): A meta-analysis. *New Phytol.* **2009**, *182*, 565–588. [[CrossRef](#)] [[PubMed](#)]
54. Santiago, L.S.; Goldstein, G.; Meinzer, F.C.; Fisher, J.B.; Machado, K.; Woodruff, D.; Jones, T.; Santiago, L.; Meinzer, F. Leaf photosynthetic traits scale with hydraulic conductivity and wood density in Panamanian forest canopy trees. *Oecologia* **2004**, *140*, 543–550. [[CrossRef](#)] [[PubMed](#)]
55. Campanello, P.I.; Gatti, M.G.; Goldstein, G. Coordination between water-transport efficiency and photosynthetic capacity in canopy tree species at different growth irradiances. *Tree Physiol.* **2008**, *28*, 85–94. [[CrossRef](#)] [[PubMed](#)]
56. Zhang, J.-L.; Cao, K.-F. Stem hydraulics mediates leaf water status, carbon gain, nutrient use efficiencies and plant growth rates across dipterocarp species. *Funct. Ecol.* **2009**, *23*, 658–667. [[CrossRef](#)]
57. Maherali, H.; Delucia, E.H. Influence of climate-driven shifts in biomass allocation on water transport and storage in ponderosa pine. *Oecologia* **2001**, *129*, 481–491. [[CrossRef](#)]

58. Fan, D.-Y.; Jie, S.-L.; Liu, C.-C.; Zhang, X.-Y.; Xu, X.-W.; Zhang, S.-R.; Xie, Z.-Q. The trade-off between safety and efficiency in hydraulic architecture in 31 woody species in a karst area. *Tree Physiol.* **2011**, *31*, 865–877. [[CrossRef](#)]
59. Ackerly, D.J. Functional strategies of chaparral shrubs in relation to seasonal water deficit and disturbance. *Ecol. Monogr.* **2004**, *74*, 25–44. [[CrossRef](#)]
60. Yates, C.; Hobbs, R.; Bell, R. Factors limiting the recruitment of *Eucalyptus salmonophloia* in remnant woodlands. I. pattern of flowering, seed production and seed fall. *Aust. J. Bot.* **1994**, *42*, 531–542. [[CrossRef](#)]
61. Fensham, R.J.; Fairfax, R.J.; Ward, D.P. Drought-induced tree death in savanna. *Glob. Chang. Biol.* **2009**, *15*, 380–387. [[CrossRef](#)]
62. Bennett, A.C.; McDowell, N.G.; Allen, C.D.; Anderson-Teixeira, K.J. Larger trees suffer most during drought in forests worldwide. *Nat. Plants* **2015**, *1*, 15139. [[CrossRef](#)]



© 2019 by the authors. Licensee MDPI, Basel, Switzerland. This article is an open access article distributed under the terms and conditions of the Creative Commons Attribution (CC BY) license (<http://creativecommons.org/licenses/by/4.0/>).